Resolution of the Four Hemes of Cytochrome *c*554 from *Nitrosomonas europaea* by Redox Potentiometry and Optical Spectroscopy†

David M. Arciero,‡ Michael J. Collins,‡,§ Jean Haladjian,∥ Pierre Bianco,∥ and Alan B. Hooper*,‡

Department of Genetics and Cell Biology, University of Minnesota, St. Paul, Minnesota 55108, and Laboratorie de Chimie et Electrochimie des Complexes, Universite de Provence, Place Victor Hugo, 13331 Marseille Cedex 3, France

Received July 5, 1991; Revised Manuscript Received September 9, 1991

ABSTRACT: The electrochemical behavior of tetraheme cytochrome *c*554 from *Nitrosomonas europaea* has been studied by thin-layer spectroelectrochemistry, cyclic voltammetry, differential pulse voltammetry, and alternating current voltammetry. Three redox couples were detected. Midpoint potentials for the high-, intermediate-, and low-potential couples are +47, −147, and −276 mV, respectively, from the spectroelectrochemical measurements and +50, −120, and −225 mV, respectively, from the voltammetry measurements. A coulometric titration shows that two electrons are taken up by the high-potential couple and one each is taken up by the intermediate- and low-potential couples. Results from the spectroelectrochemical titration at carefully chosen wavelengths indicate that the intermediate- and low-potential couples obey simple Nernstian behavior. The electrochemical behavior of the high-potential couple is apparently not truly Nernstian but is most consistent with two sites exhibiting slight positive cooperativity. Spectral changes associated with the three couples reveal distinctive features in the reduced-*minus*-oxidized difference spectra. The difference spectrum of the high-potential pair of hemes suggest a mixture of a high-spin heme and a low-spin heme with maxima at 424 and 432 nm. The difference spectrum of the intermediate-potential heme is low spin with a split Soret with maxima at 414 and 424 nm. The difference spectrum of the low-potential heme also shows a split Soret with maxima at 418 and 432 nm.

Cytochrome *c*554 functions in the pathway of ammonia oxidation in *Nitrosomonas europaea*. In this pathway, ammonia monooxygenase (AMO)[1] ($NH_3 + O_2 + 2H^+ + 2e^- \rightarrow NH_2OH + H_2O$) and hydroxylamine oxidoreductase (HAO) ($NH_2OH + H_2O \rightarrow NO_2^- + 5H^+ + 4e^-$) act in concert to metabolize NH_3 as the sole source of energy for the organism. The catalytic functions of AMO and HAO are interdependent since AMO provides the substrate, NH_2OH, to HAO and HAO, in turn, provides the two electrons required by the monooxygenase. The two additional electrons from HAO are apparently passed to the electron transfer chain leading to the terminal oxidase. Overall, the system leads to the synthesis of ATP and reducing equivalents for growth.

While the exact role of cytochrome *c*554 in the oxidation of ammonia has not been known with certainty, it most likely participates as an electron transfer catalyst. The initial report on this cytochrome described its ability to act as an electron acceptor during the oxidation of NH_2OH by HAO as well as its ability to act catalytically, during the same reaction, to reduce cytochrome *c*552, a monoheme cytochrome also present in *N. europaea* (Yamanaka & Shinra, 1974). In the following paper (Arciero et al., 1991), kinetic analysis demonstrates the formation of a stable complex between HAO and cytochrome *c*554 during turnover of NH_2OH by HAO. In this complex, electrons from hydroxylamine can be passed to cytochrome *c*554 by HAO more rapidly than they are abstracted from the substrate by HAO (Hooper et al., 1984). Cytochrome *c*554 is also able to promote ammonia-oxidizing activity, possibly as an electron donor to AMO, by a membrane fraction obtained from *N. europaea* (Suzuki & Kwok, 1982).

Initially described as a diheme cytochrome (Yamanaka & Shinra, 1974), cytochrome *c*554 was subsequently shown to actually contain four c-type hemes on a single polypeptide of 25 kDa (Andersson et al., 1986). A comprehensive study comparing the optical, EPR, and Mossbauer properties of cytochrome *c*554 concluded that all four hemes interact magnetically at neutral pH but did not clearly indicate individual spin states of the oxidized hemes. Mossbauer spectroscopy indicated a mix of low-spin to high-spin iron in the protein at neutral pH in the ratio of approximately 3:1. Optical spectra for the ferrous cytochrome are consistent with such a low-spin/high-spin mix. A Soret maximum is observed at 418 nm together with a distinct shoulder at approximately 430 nm. Surprisingly, however, EPR spectra did not delineate either high-spin or low-spin hemes but instead were consistent with a complex spin-paired system. This cytochrome maintains the same spectral properties over a broad pH range but converts into a predominantly high-spin system at low pH (<4.2) and a low-spin system at high pH (>9.5). NMR spectra of cytochrome *c*554 at neutral pH resolved only four resonances in the low-field region at 64, 78, 81, and 93 ppm (Petersson & Andersson, 1987), a range that is typical for ring methyls of high-spin ferric hemoproteins. This strongly suggested the presence of a single high-spin heme in cytochrome *c*554. The low-spin ferric heme region of the NMR spectrum between 10 and 26 ppm was much more complex, suggesting the

† This work was supported by Grant NSF/DMB-9019687.

* Author to whom correspondence should be addressed.

‡ University of Minnesota.

§ Present address: Department of Chemistry, Viterbo College, La-Crosse, WI 54601.

∥ Universite de Provence.

[1] Abbreviations: AMO, ammonia monooxygenase; HAO, hydroxylamine oxidoreductase; ATP, adenosine triphosphate; EPR, electron paramagnetic resonance; NMR, nuclear magnetic resonance; OTTLE, optically transparent thin-layer electrode; CV, cyclic voltammetry; ACV, alternating current voltammetry; DPV, differential pulse voltammetry; NHE, normal hydrogen electrode; lpi, lines per inch.

0006-2960/91/0430-11459$02.50/0

presence of multiple low-spin hemes. It was concluded that cytochrome *c*554 contains one individual high-spin ferric heme and three slightly different low-spin ferric hemes and not four hemes each in a high-spin/low-spin equilibrium.

An early redox titration of cytochrome *c*554, before it was known to be a tetraheme cytochrome, suggested that all hemes had a midpoint potential (E_{m7}) of +20 mV (Miller & Wood, 1982). However, because of the complex nature of cytochrome *c*554 evident from the physical studies described above, as well as asymmetric absorption changes and multiphasic kinetics noted during both reduction with dithionite (DiSpirito et al., 1987) and electron transfer from NH_2OH-reduced HAO (Arciero et al., 1991), a reexamination of the electrochemical behavior of cytochrome *c*554 was clearly warranted. We report here the results obtained using redox mediators and an optically transparent thin-layer electrode (OTTLE) cell (Murray et al., 1967), which allows us to monitor the spectroscopic changes occurring during the potentiometric titration, as well as standard voltammetric techniques [cyclic voltammetry (CV), differential pulse voltammetry (DPV), and alternating current voltammetry (ACV)] using a variety of electrodes in the absence of redox mediators.

Materials and Methods

Materials. Cytochrome *c*554 was prepared from *N. europaea* somewhat differently from the procedure described previously (Yamanaka & Shinra, 1974). A cell-free extract, obtained from *N. europaea* by centrifugation after three freeze–thaw cycles to disrupt membranes, was routinely fractionated with ammonium sulfate sequentially at 40, 50, 60, 80, and 100% levels of saturation. The supernatant remaining after the 100% ammonium sulfate cut contains the cytochrome *c*554. This supernatant was diluted slightly to lower the ammonium sulfate concentration to approximately 80–90% saturation. The cytochrome *c*554 was then adsorbed onto a column of octyl-Sepharose (Pharmacia) (4.0 cm × 17 cm) equilibrated with 50 mM KPO_4 buffer, pH 7.5, containing 90% saturated ammonium sulfate. After the column was washed with 2 volumes of the equilibration buffer, cytochrome *c*554 was eluted from the column with 50 mM KPO_4 buffer, pH 7.5, containing no ammonium sulfate. After dialysis vs 20 mM KPO_4 buffer, pH 7.5, cytochrome *c*554 was adsorbed onto a column of Amberlite CG-50 (Rohm & Haas) cation-exchange resin (2.5 cm × 18 cm) equilibrated with the dialysis buffer. The column was then washed with the equilibration buffer (2–4 volumes), and then cytochrome *c*554 was eluted with a linear KCl gradient from 0.0 to 1.0 M (500 mL × 500 mL). If necessary, cytochrome *c*554 was further purified by gel filtration on a column of Sephadex G-100 (Pharmacia) (2.5 cm × 110 cm) equilibrated with 50 mM KPO_4 buffer, pH 7.5, containing 0.1 M KCl. The purity of cytochrome *c*554 was monitored spectroscopically. Fully purified cytochrome *c*554 has an A_{406} vs A_{280} ratio of 6.6.

Dyes used as redox mediators included 1,2-naphthoquinone-4-sulfonic acid (E_{m7} = +215 mV), phenazine methosulfate (E_{m7} = +80 mV), gallocyanine (E_{m7} = +21 mV), pyocyanine (E_{m7} = −34 mV), indigo-5,5-disulfonic acid (E_{m7} = −125 mV), anthraquinone-2-sulfonic acid (E_{m7} = −230 mV), safranine O (E_{m7} = −290 mV), benzyl viologen (E_{m7} = −350 mV), and methyl viologen (E_{m7} = −430 mV) and were obtained from Aldrich or Sigma.

Spectropotentiometric and Coulometric Measurements. Apparatus. The optically transparent thin-layer electrode (OTTLE) cell used in this investigation was constructed basically as originally described (Heineman et al., 1975). The path length was determined to be 0.0136 cm. The working, indicator, and reference electrodes were the 500 1pi gold mesh minigrid (Buckbee-Mears Co., St. Paul, MN), Pt wire, and saturated calomel (Radiometer America Inc., Westlake, OH) electrodes, respectively. Both the spectropotentiometric and coulometric titrations were carried out using a Bioanalytical Systems CV-27 voltammograph. Potentials were monitored using either a Soar ME-530 digital multimeter or a Data Precision Model 245 digital multimeter. Spectra were recorded with a Hewlett Packard 8452A diode array spectrometer and stored automatically on a Hewlett Packard 9000 Series 300 computer using their Chemstation software. Spectral subtractions were carried out using the same software.

Methods. The OTTLE experiments were caried out in 50 mM KPO_4/100 mM KCl buffer at pH 7.0. For the spectropotentiometric titration using the OTTLE cell, spectra were recorded at resting potential and at 10-mV increments between +175 and −405 mV for both the dye solution alone and the cytochrome *c*554/dye mixture. The experiment was carried out in both reductive and oxidative modes. In the reductive titration, the potential was initially poised at +175 mV. Spectra were monitored as the current dropped from its initial value. Generally, by the time current dropped to a value below 1.5 μA (approximately 5–10 min), spectral changes were no longer evident and a final spectrum was recorded and stored. In the oxidative mode, the potential was initially poised at −405 mV and the system was allowed to equilibrate for 2 h. After an initial spectrum was taken, the potential was decreased in 10-mV steps while the current was monitored. When the current dropped to 0 mA (approximately 5–10 min) in each step a spectrum was recorded and stored. Despite its structural complexity, cytochrome *c*554 proved to be a very well-behaved electrochemical system when it was monitored optically. Reversibility of the first redox couple was tested by first carrying out a reductive titration from +175 to −105 mV followed by an oxidative titration back to +175 mV. A comparison of absorbance–potential curves and Nernst plots from both the reductive and oxidative titrations showed nearly superimposable traces and midpoint potentials differing by less than 5 mV. Furthermore, cytochrome *c*554 could be cycled between the fully oxidized and fully reduced states numerous times with no discernible alterations in the optical properties.

A coulometric titration was carried out on the dye mixture alone and a cytochrome *c*554/dye mixture at potentials between −355 and +245 mV. The dyes used were 1,2-naphthoquinone-4-sulfonic acid, indigo-5,5-disulfonic acid, and methyl viologen at a final concentration of 0.1 mM. The system was initially poised at −355 mV and allowed to equilibrate for 2 h. A spectrum was then recorded. The potential was then reset to either −25 mV or +245 mV while the current was integrated until it dropped to residual values. Spectra were again recorded. The sample initially reset to −25 mV was then reset again to +245 mV while the current was again integrated. A final spectrum was then recorded after the current dropped once again to residual values. Because of the choice of dyes, this titration of cytochrome *c*554 was only applicable in the oxidative mode. In the reductive mode, the system could be poised at the intermediate −25-mV potential. However, cytochrome *c*554 was not reduced at a significant rate under these conditions and the spectrum of cytochrome *c*554 at −25 mV reached in a reductive titration was barely distinguishable from fully oxidized cytochrome *c*554. This observation illustrates a potential deficiency in the four-dye mixture believed to give adequate control over a broad potential range (Meckstroth et al., 1981); large windows exist between the useful voltage-buffering ranges of the dyes where

potential may actually be controlled but insufficient amounts of titrating species exist to equilibrate the unknown species with the dyes at an appreciable rate.

Data Analysis. Dye spectra were subtracted from the corresponding spectra of the cytochrome *c*554/dye mixture. The dye-corrected spectra of cytochrome *c*554 was then used to generate the reduced-*minus*-oxidized spectra shown in this paper as well as the data taken to calculate midpoint potentials and *n* values. Theoretical curves were constructed from the Nernst equation assuming Nernstian behavior for a $1e^-$ system using an Apple Macintosh SE/30 computer and Cricket graph software. Data points were generated at 5-mV intervals. Midpoint potentials and amplitudes of theoretical curves were set using best-fit values derived from the actual data. Multiphasic theoretical curves were then constructed from summation of the individual curves. The best fit to the data could be achieved using *n* values derived from the actual data for each transition or by generating data points at smaller potential intervals (1–2 mV). However, the objective of the simulations was to assess how well the data resembled Nernstian behavior rather than to try to achieve a best fit to the data.

Voltammetric Measurements. Electrochemical experiments involving cyclic voltammetry (CV), differential pulse voltammetry (DPV), and alternating current voltammetry (ACV) were performed on 50 μM cytochrome *c*554 in 50 mM KPO_4, pH 7.0, buffer. The working electrode was either the polished pyrolytic graphite or the aldrithiol-modified gold electrode (Taniguchi et al., 1982). The aldrithiol-modified gold electrode was prepared as described previously for cytochrome *c* (Haladjian et al., 1983) by immersing the gold surface in a solution of 1 mM aldrithiol [bis(4-pyridyl) disulfide], rinsing, and then transferring to a solution of cytochrome *c*554. The mercury electrode proved to be unsuitable for cytochrome *c*554 because it resulted in adsorption of the protein to the electrode surface. CV experiments were performed using a PAR 173 potentiostat and a PAR 175 universal programmer. DPV experiments were performed using a PAR 174A polarographic analyzer. ACV experiments were carried out using an EG&G PAR 273 Potentiostat and an EG&G PAR 5208 lock-in analyzer, both controlled by an IBM XT microcomputer and EG&G PAR Head Start software. Data was collected using a Sefram X-Y chart recorder.

All measurements were made at room temperature. All potentials are given vs the NHE.

Results

OTTLE Experiments. Using cytochrome *c*554 at +155 mV as the oxidized cytochrome, a series of reduced-*minus*-oxidized spectra for cytochrome *c*554 poised at 10-mV increments were generated between +155 and −395 mV. This progressive reduction of cytochrome *c*554 was observed to occur in three distinct steps. To best illustrate the spectral changes associated with these three transitions, an oxidized spectrum was chosen for the second and third transitions such that the previous transition contributed less than 2% to the spectral changes shown for that particular transition. Likewise, reduced spectra were chosen by the same criteria. Thus, for the reduced-*minus*-oxidized spectra shown in Figure 1, well-defined isosbestic points are observed, indicating that each transition represents the conversion of a single species from the oxidized state to the reduced state. The absence of isosbestic points in the α,β region in Figure 1A is due to an incomplete subtraction of the gallocyanine spectrum. Gallocyanine ($E^{\circ\prime}$ = +21 mV) is reduced in this potential range with broad spectral changes centered at 590 nm. In second-derivative spectra, where sharper transitions are enhanced and broad transitions contribute very little to the spectrum, clear isosbestic points are observed for cytochrome *c*554 in this region.

Table I: Coulometric Titration of Cytochrome *c*554[a]

reaction mixture	endpoint potentials (mV)[b] −355/+245	−355/−025	−025/+245
dye	0.43	0.31	0.39
*c*554 + dye	2.70	1.23	1.53
*c*554(measured)	2.27 (23.5)	0.92 (9.5)	1.14 (11.8)
*c*554(expected)	2.04 (21.2)	1.02 (10.6)	1.02 (10.6)

[a] See Materials and Methods for details. Values in the table are given in millicoulombs. Parenthetical values are in nanomoles. [b] Versus NHE.

Table II: Values of Δε (in mM^{-1} cm^{-1}) for Hemes of Cytochrome *c*554[a]

wavelength (nm)	transition 1	transition 2	transition 3
324	20.9	16.1	13.3
388	−81.3	−25.6	−18.0
398	−64.0	−38.9	−34.1
402	−53.3	−37.9	−39.8
413	IP[b]	42.2	33.2
414	11.9	48.6	42.7
416	46.7	44.8	61.4
418	87.7	37.9	60.6
419	104.3	37.9	58.1
424	116.2	73.5	39.1
432	97.7	10.2	41.5
436	64.0	IP[b]	21.3
440	28.0	−9.0	IP[b]
446	IP[b]	−10.9	−11.6
522	1.8	5.2	5.6
552	8.5	20.9	25.8

[a] Values were extracted from the reduced-*minus*-oxidized spectra shown in Figure 1. Underlined values indicate maxima in the reduced-*minus*-oxidized spectra for each particular transition. [b] Isosbestic point.

Dye-subtracted spectra of cytochrome *c*554 poised at +155, −385, −25, and −205 mV are shown in Figure 2A. These potentials correspond to plateau regions at the beginning, at the end, between transitions 1 and 2, and between transitions 2 and 3, respectively, in the spectroelectrochemical titration. The resulting reduced-*minus*-oxidized spectra corresponding to these three transitions are overlaid in Figure 2B. Figure 2C highlights the spectral differences in the Soret region for the three transitions.

Spectral changes associated with the first transition are approximately twice as great as for the second or third transitions, suggesting that there are two, one, and one hemes reduced in each of the three transitions. To test this, a coulometric titration was carried out, the results of which are shown in Table I. Since only the first two transitions are separated by a significant plateau, the number of electrons taken up by the first transition, the second and third transitions combined, and all three transitions together, was determined. There was 5.3 nmol of cytochrome *c*554 undergoing reduction in the OTTLE cell (on the basis of a calculation of effective cell volume of 20.5 μL and a cytochrome *c*554 concentration of 0.26 mM). From the number of coulombs taken up in the three potential ranges, there are thus two electrons taken up by cytochrome *c*554 in the first transition, two electrons in transitions two and three combined, and four electrons in the complete reduction.

It can be seen from a comparison of the reduced-*minus*-oxidized spectra of Figure 2B,C that all four hemes have unique spectral features. Table II lists maxima and minima along with the associated Δε values as well as isosbestic points for each of the three transitions. Spectral features of the

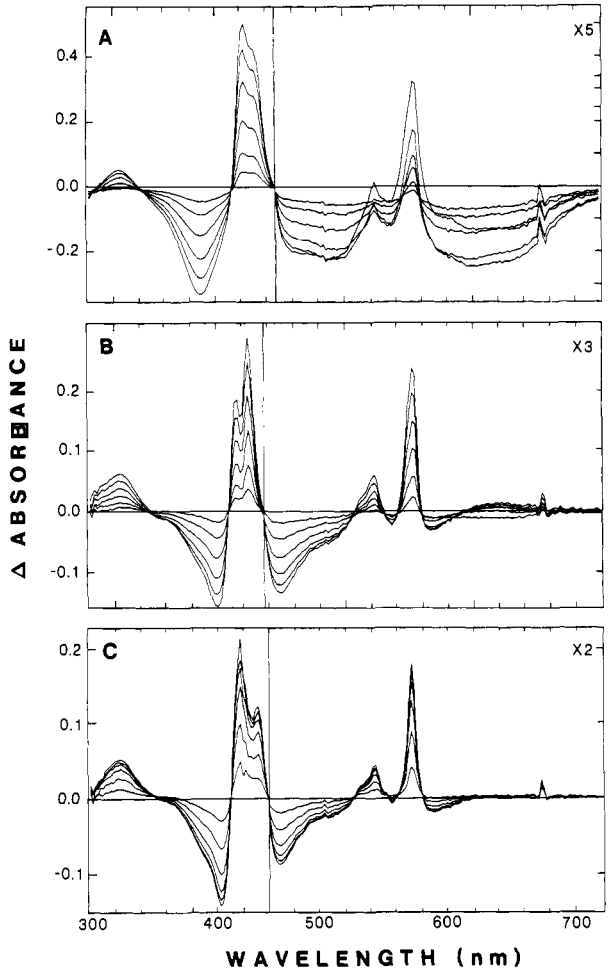

FIGURE 1: Reduced-*minus*-oxidized difference spectra of 0.26 mM cytochrome *c*554 measured for different potential ranges and showing titration of three electrochemically distinguishable heme species. (A) Oxidized spectrum recorded at +155 mV, reduced spectra at −25, −5, +15, +35, +55, +75, +95, and +115 mV. (B) Oxidized spectrum recorded at −65 mV, reduced spectra at −205, −185, −165, −145, −125, −105, and −85 mV. (C) Oxidized spectrum recorded at −245 mV, reduced spectra at −385, −365, −345, −325, −305, −285, and −265, mV. Conditions were as described under Materials and Methods.

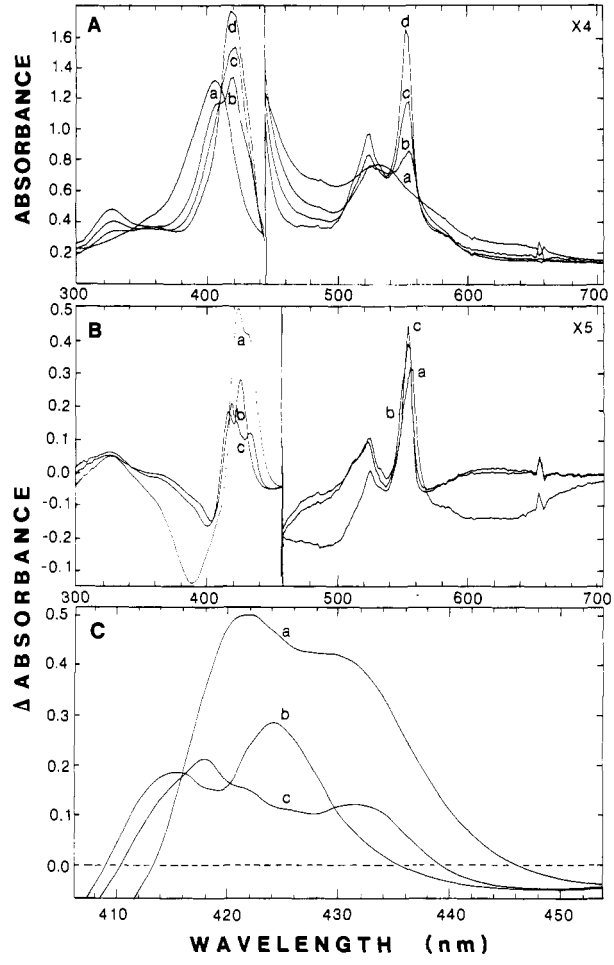

FIGURE 2: Optical spectra of 0.26 mM cytochrome *c*554 poised at selected potentials using the OTTLE cell (A) and reduced-*minus*-oxidized spectra of the three electrochemically distinguishable species (B). Conditions were as described under Materials and Methods. (A) Oxidized cytochrome *c*554 at +155 mV (a), partially reduced cytochrome *c*554 at −25 mV (b) and −205 mV (c), and fully reduced cytochrome *c*554 at −385 mV (d). (B) Spectra of −25 mV minus +145 mV (a), −205 mV minus −65 mV (b), and −385 mV minus −245 mV (c) species. (C) Expanded spectra of the Soret bands of the three reduced-*minus*-oxidized species. Spectra were smoothed by using a cosine fitting routine to interpolate data between actual data points collected at 2-nm intervals.

high-potential hemes 1 and 2, which change simultaneously in response to redox potential, are consistent with the two hemes being a mix of high-spin and low-spin hemes. Soret bands of high-spin ferric and ferrous hemes are typically near 390 and 430 nm, respectively, in contrast to those of low-spin ferric and ferrous hemes which are found near 406 and 418 nm, respectively. It has been established by Mossbauer spectroscopy that approximately 25% of the hemes in cytochrome *c*554 are high spin (Andersson et al., 1986), while optical spectroscopy of the fully reduced cytochrome clearly indicates a shoulder on the Soret peak near 430 nm (Figure 2A). Thus, we take the Soret bands in the reduced-*minus*-oxidized difference spectra at 424 and 432 nm to represent the low-spin and high-spin hemes, respectively (Figure 2C). A second spectral feature previously attributed to the high-spin heme of cytochrome *c*554 and observed here in this first transition is the broad absorbance decrease near 645 nm (Figure 2A,B). The heme reduced in transition 2 is clearly low spin with split Soret maxima at 414 and 424 nm in the reduced-*minus*-oxidized difference spectra. The lowest potential heme also appears to be a mix of high-spin and low-spin hemes having maxima near 432 and 416 nm, respectively. The four electrochemically unique hemes are further distinguished by slight differences in the α band (Figure 2B). Peak maxima appear to be at 554 nm for the first transition and at 552 nm for the second and third transitions. Surprisingly, intensities of the α bands for the three transitions are roughly equal with line widths that are only slightly different. Reduction of two hemes in the first transition would be expected to result in twice the intensity of the α band or else more significant peak broadening for this transition.

Representative absorption–potential curves derived from the data at selected wavelengths are presented in Figure 3. Wavelengths were chosen to satisfy subjective criteria that would allow (1) isolation of two of the three transitions free from the third, (2) isolation of high-spin hemes from low-spin hemes (and vice versa), and (3) comparison of Nernst numbers derived from different absorption bands within the entire spectrum. Since each of the three transitions has a unique isosbestic point in the 440-nm region (Table II), we have used 436, 440, and 446 nm to isolate two of the transitions free from the third, thus allowing for a more reliable assignment of midpoint potentials and *n* values from Nernst plots. In addition, at 436 nm the high-spin hemes are effectively isolated from the low-spin hemes whereas at 413 nm the low-spin hemes are being preferentially monitored. At 324 and 398

Table III: Midpoint Potentials and Nernst Values for Hemes of Cytochrome *c*554 Determined by Spectroelectrochemistry[a]

	transition 1		transition 2		transition 3	
wavelength (nm)	$E^{\circ\prime}$ (mV)	slope	$E^{\circ\prime}$ (mV)	slope	$E^{\circ\prime}$ (mV)	slope
324	43	48	−153	53	−283	48
398	51	55	−146	49	−281	50
413			−151	59[b]	−274	56[b]
418	44	47	−151	61	−275	55
424	46	49[b]	−149	55[b]	−273	55[b]
432	47	50[b]	−150	46	−271	62[b]
436	47	51			−267	62
440	46	50	−137	55		
446			−136	48	−282	49
552	49	48[b]	−149	55[b]	−278	53[b]
av	47	49 (1.21)	−147	56 (1.05)	−276	56 (1.05)

[a] Values of midpoint potentials and slopes were derived from Nernst plots. [b] Values used in determining averages.

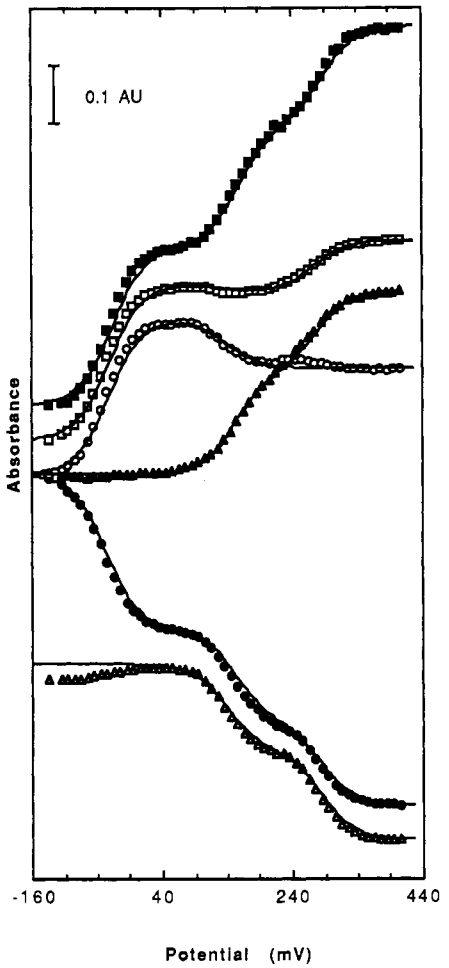

FIGURE 3: Absorption–potential plots for cytochrome *c*554 at selected wavelengths. Absorption data was taken from reduced-*minus*-fully oxidized spectra over the entire potential range. Some plots have been expanded and/or offset. Selected wavelengths included 324-*minus*-348 nm (■) ($\Delta A \times 3.1$), 398 nm (●), 413 nm (▲), 436 nm (□), 440 nm (○) ($\Delta A \times 2.3$), and 446 nm (△) ($\Delta A \times 3.2$). Smooth lines through the absorption data at each wavelength are simulated curves for a three-component system using midpoint potentials (Table III) and extinction coefficients (Table II) derived from the data and assuming Nernstian behavior (n = 1 system).

nm all three transitions are being monitored. Corresponding data from the 552-nm absorption band are not shown because of the interference in this part of the spectrum from the reduction of gallocyanine during the first transition (Figure 1A).

The corresponding Nernst plots derived from the data in Figure 3 were found to be linear at all chosen wavelengths for all three transitions. Midpoint potentials, slopes, and n values obtained from linear least-squares fit to the data at several wavelengths are given in Table III. Values for the 552-nm absorption band are approximate, being obtained by constructing an artificial base line between 540 and 560 nm (approximate isosbestic points for the three transitions). Midpoint potentials and slopes are given for each of the transitions at all of the wavelengths listed in Table III. It is clear in Table III that midpoint potentials for the three transitions are relatively independent of the wavelength monitored. It is equally apparent that slopes take on a range of values depending on the wavelength. Using all of the data to obtain a simple average for the slope for each of the transitions would lead to a slight misrepresentation of the actual values; because all four hemes in cytochrome *c*554 have unique spectral features, some values should be more reliable than others and are so designated in the table. Some wavelengths, for example, fall on steeply sloping lines rather than at absorption maxima. At other wavelengths, extinction coefficients are small for some transitions. Therefore, only values at those wavelengths that would typically be monitored in a spectroelectrochemical experiment were arbitrarily chosen to obtain the averages listed in Table IV.

Table IV: Comparison of Midpoint Potentials (vs NHE) of Cytochrome *c*554 Obtained from Spectropotentiometric and Voltammetric Measurements

technique	cyt *c*554 (μM)	E_1'	E_2'	E_3'
OTTLE[a]	260	47 ± 4	−147 ± 5	−276 ± 7
voltammetry[b]	50	50 ● 10	−120 ± 20	−225 ● 40

[a] The working electrode was a gold minigrid using redox mediator dyes. [b] The working electrodes were a pyrolytic graphite (CV and DPV) or an aldrithiol-modified gold electrode (ACV).

Voltammetric Experiments. Cyclic and differential pulse voltammetry curves at the pyrolytic graphite electrode are shown in Figure 4. Three couples (1c–1a, 2c–2a, 3c–3a) are observed in Figure 4A and three corresponding DPV peaks (1, 2, and 3) are seen in Figure 4B. The existence of three reduction–oxidation steps was verified by ACV as shown by the forward and backward traces of Figure 4C.

The aldrithiol-modified gold electrode was used to study the promoting effect of aldrithiol on the electrochemistry of cytochrome *c*554, and the results are shown in Figure 5. A fast CV couple can be observed in Figure 5A, which corresponds to the reduction–oxidation ACV peak at E_p = 50 mV in Figure 5B. Repetitive scanning can be performed several times without any modification of the electrochemical response, thus suggesting that no degradation accompanies the first reduction step. The results at the aldrithiol-modified gold electrode are consistent with those obtained at graphite, but the experiments at the aldrithiol-modified gold electrode provide a more accurate determination of the first redox couple. Redox potentials corresponding to the three steps are given in Table IV

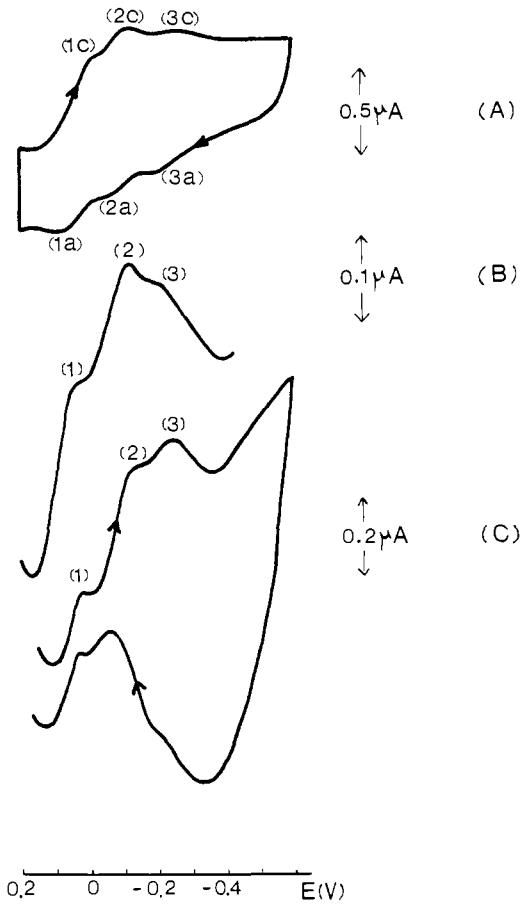

FIGURE 4: Cyclic voltammogram (A), differential pulse voltammogram (B), and cyclic alternating current voltammogram (C) at the pyrolytic graphite electrode of 50 μM cytochrome *c*554 in 50 mM KPO_4 buffer at pH 7.0. CV scan rate = 10 mV s^{-1}. DPV experimental conditions: scan rate = 5 mV s^{-1}; pulse repetition rate = 0.5 s^{-1}; $\Delta E = -50$ mV. ACV experimental conditions: ΔE = 10 mV rms; f = 30 Hz.

with some uncertainty on E_3' due to a rather poor reversibility of the third step that tends to disappear upon repetitive scanning.

Discussion

Both the spectroelectrochemical and voltammetric experiments clearly show the existence of three redox couples in cytochrome *c*554. As noted in Table IV, close agreement is found for the high-potential redox couple from both techniques. A slight deviation is apparent for the midpotential redox couple, with the difference becoming more pronounced for the low-potential couple. In the voltammetric experiments, this third redox couple is also the least reliable due to a lack of repeated reversibility. The basis for the slight discrepancy is unknown but possibly arises from the different properties being monitored in the two experimental approaches. In the OTTLE experiments, since actual spectroscopic changes are being measured for each transition, microscopic potentials are being measured for each of the hemes, whereas in the voltammetric experiments measurements are macroscopic potentials. The latter will be identical to the microscopic potentials only when differences in midpoint potentials of the individual centers in a multicenter system are large enough so that the individual centers are electrochemically isolated from each other (Sokol et al., 1980). In cytochrome *c*554, it is clear that the midpotential and low-potential redox couples do not meet this criteria. An alternative explanation could be a difference in experimental conditions. The two sets of experiments were performed under somewhat different buffer conditions (100 mM KCl and several redox dyes are present in the buffer used in the OTTLE experiments). Moreover, slightly different cytochrome concentrations (0.25 mM in OTTLE experiments vs 0.05 mM in voltammetric experiments) were used.

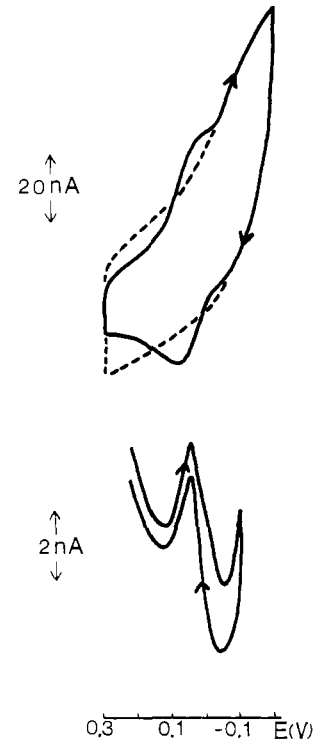

FIGURE 5: Cyclic voltammogram (A) and alternating current voltammogram (B) at the aldrithiol-modified gold electrode of cytochrome *c*554. Conditions were otherwise identical to those in Figure 4.

The spectroelectrochemical study of a complex, multiheme cytochrome such as cytochrome *c*554 using the OTTLE cell is somewhat more informative than the voltammetric experiments in that it allows us to correlate the electrochemical behavior with distinct spectral transitions, thereby allowing us to resolve individual hemes on the basis of differences in both their spectroscopic and potentiometric properties. The OTTLE study is most consistent with the interpretation that cytochrome *c*554 is, indeed, a tetraheme cytochrome. The coulometric titration indicates that two heme equivalents are reduced during the first spectral transition with an additional two hemes reduced during the second and third transitions combined. The two high-potential hemes reduced in the first spectral transition appear to be a mix of high-spin and low-spin species. However, the exact ratio of high-spin to low-spin hemes is not established here. In addition, this study does not differentiate between one heme being high-spin and the other being low-spin or the possibility that both hemes exist in a high-spin/low-spin equilibrium. The assignment that one heme is high spin while the other is low spin is reasonably valid, nevertheless, on the basis of previous Mossbauer (Andersson et al., 1986) and NMR (Petersson & Andersson, 1987) investigations. Furthermore, it is demonstrated in the following paper (Arciero et al., 1991) that the two hemes of the first redox couple can be individually isolated by monitoring at either 418 or 436 nm. It is clear from Table III that midpoint potentials and slopes obtained from the Nernst plots for the first redox couple at either wavelength are essentially identical; i.e., both have the same midpoint potential and both display non-Nernstian behavior. This would suggest some special interaction between these two hemes that bears further study. The remaining two hemes of cytochrome *c*554 each have unique midpoint potentials and spectroscopic features. While

the midpotential heme is clearly low-spin, the low-potential heme may also be a mix of low-spin and high-spin species. This is based on the presence of two Soret bands at 418 and 430 nm for this transition. Thus, in the absence of other criteria, and in an attempt to simplify future references to the individual hemes of cytochrome c554, the four hemes are therefore designated as heme $c(+47)_{hs}$, heme $c(+47)_{ls}$, heme $c(-147)$, and heme $c(-276)$ from the high-potential, medium-potential, and low-potential regions, respectively.

Heme $c(-147)$ and heme $c(-276)$ appear to obey simple Nernstian behavior for a one-electron acceptor on the basis of identical average slopes of 56. The high-potential pair, heme $c(+47)_{hs}$ and heme $c(+47)_{ls}$, clearly deviates from Nernstian behavior in a manner that leads to positive cooperativity in reduction of the two hemes. The physical basis for this cooperativity is unknown but may exist because of the apparent function of cytochrome c554 as a two-electron carrier in *N. europaea* (Arciero et al., 1991).

A previous report investigating the kinetics of reduction of ferric cytochrome c554 by dithionite used rapid-scan absorption spectra in an attempt to differentiate hemes in cytochrome c554 (DiSpirito et al., 1987). The data suggested that there were distinct spectral bands hidden within the unusually broad Soret and α bands reported for this protein. Reduction of cytochrome c554 was monitored at 419 or 554 nm and was reportedly biphasic. Calculations, at that time, based on the amplitudes of the two phases, at 419 nm, led to the conclusion that two hemes were reduced in each phase. A comparison of that data with the data reported here suggests, however, that this conclusion was in error and that, in fact, three hemes were reduced in the fast phases and only one was reduced during the slow phase. Spectral changes reported for the slow phase (Figure 2B,D from that report) are virtually identical with the reduced-*minus*-oxidized spectrum for the low-potential heme of cytochrome c554 shown in Figure 2B in this report. This low-potential heme has maxima in the reduced-*minus*-oxidized Soret spectrum at 418 and 432 nm as does the heme species reduced by dithionite in the slow phase. Furthermore, positions of the isosbestic cross-over points at 410 and 440 nm are virtually identical for the two sets of experiments. In addition, the clean isosbestic points obtained for the reduction by dithionite of the heme species in the slow phase suggests that only a single species was undergoing reduction. In contrast, spectral changes associated with the fast phase for the reduction of cytochrome c554 by dithionite do not closely resemble the reduced-*minus*-oxidized spectrum for reduction of the two high-potential hemes but can be more readily duplicated by combining reduced-*minus*-oxidized spectra from both the high- and medium-potential transitions (data not shown). Spectral changes for the fast phase show a clear shoulder near 416 nm and a major band at 425 nm. A reduced-*minus*-oxidized spectrum for the two high-potential hemes (Figure 2B; this report) does not show this shoulder at 416 nm. Also, no clean isosbestic points are observed in the fast phase indicating the presence of multiple species undergoing reduction by dithionite. Finally, using the $\Delta\epsilon$ values at 419 nm from Table III, a 2:1 ratio of amplitudes would have been expected on the basis of this revised interpretation. This is reasonably close to the ratio observed in several of the figures presented previously (DiSpirito et al., 1987).

Acknowledgments

We thank Candace Pilon, Erica van Dyck, and Jeff Strom for their expertise in maintaining and growing cultures of *N. europaea*.

Registry No. Cytochrome c554, 52932-67-9; heme c, 26598-29-8.

References

Andersson, K. K., Lipscomb, J. D., Valentine, M., Münck, E., & Hooper, A. B. (1986) *J. Biol. Chem. 261*, 1126–1138.

Arciero, D. M., Balny, C., & Hooper, A. B. (1991) *Biochemistry* (following paper in this issue).

DiSpirito, A. A., Balny, C., & Hooper, A. B. (1987) *Eur. J. Biochem. 162*, 299–304.

Haladjian, J., Bianco, P., & Pilard, R. (1983) *Electrochim. Acta 28*, 1823–1830.

Heineman, W. R., Norris, B. J., & Goelz, J. F. (1975) *Anal. Chem. 47*, 79–84.

Hooper, A. B., Tran, V. M., & Balny, C. (1984) *Eur. J. Biochem. 141*, 565–571.

Meckstroth, M. L., Norris, B. J., & Heineman, W. R. (1981) *Bioelectrochem. Bioenerg. 8*, 63–70.

Miller, D. J., & Wood, P. M. (1982) *Biochem. J. 207*, 511–517.

Murray, R. W., Heineman, W. R., & O'Dom, G. W. (1967) *Anal. Chem. 39*, 1666–1668.

Petersson, L., & Andersson, K. K. (1987) *Biochim. Biophys. Acta 915*, 261–266.

Sokol, W. F., Evans, D. H., Niki, K., & Yagi, T. (1980) *J. Electroanal. Chem. Interfacial Chem. 108*, 107–115.

Suzuki, I., & Kwok, S.-C. (1982) *Can. J. Biochem. 59*, 484–488.

Taniguchi, I., Toyosawa, K., Yamaguchi, H., & Yasukouchi, K. (1982) *J. Electroanal. Chem. Interfacial Chem. 140*, 187–195.

Tsang, D. C. Y., & Suzuki, I. (1982) *Can. J. Biochem. 60*, 1018–1024.

Yamanaka, T., & Shinra, M. (1974) *J. Biochem. (Tokyo) 75*, 1265–1273.